Computers and Fluids 158 (2017) 150–156

Contents lists available at ScienceDirect

Computers and Fluids

journal homepage: www.elsevier.com/locate/compfluid

A new variational multiscale formulation for stratified incompressible turbulent flows

J. Yan [a], A. Korobenko [b], A.E. Tejada-Martínez [c], R. Golshan [c], Y. Bazilevs [a,*]

[a] Department of Structural Engineering, University of California, San Diego, CA 92093, United States
[b] Department of Mechanical and Manufacturing Engineering, University of Calgary, Calgary Alberta Canada
[c] Department of Civil and Environmental Engineering, University of South Florida, FL 33620, USA

ARTICLE INFO

Article history:
Received 9 June 2016
Revised 14 November 2016
Accepted 7 December 2016
Available online 9 December 2016

Keywords:
Density-stratified flows
Turbulent channel flow
Self-propelled wake
RBVMS
IGA
FEM

ABSTRACT

For geophysical and environmental flows in the high-Reynolds-number regime, stable density stratification strongly affects the turbulent fluid motions. While turbulent flows, due to the presence of a cascade of spatial and temporal scales, present several challenges to accurate numerical approximation, density stratification in these flows exacerbates the situation further by suppressing vertical velocity fluctuations thereby enhancing the anisotropy of the turbulence. In this paper, based on the framework of residual-based variational multiscale (RBVMS) methods, we design a new numerical formulation for incompressible stratified flows that introduces coupling between the velocity fine scales and densityequation residual, and gives improved numerical performance as evidenced by the results of two challenging turbulent-flow simulations.

1. Introduction

Many geophysical flows in lakes, reservoirs, coastal waters, and atmosphere involve a vertically stratified fluid. Because of their ubiquity in nature, their mathematical complexity, and the challenges involved in their numerical approximation, stratified flows are of great research as well as practical interest in such areas as geophysical fluid dynamics and wind energy. Of particular interest here are stable boundary layers which can be generated, for example, by the advection of warm air over a colder surface in the atmosphere or cold water under a warmer surface in the ocean. In the ocean both temperature and salinity play important roles in determining the overall density stratification. Such flows, in the turbulent regime, are already numerically challenging due to the presence of a cascade of spatial and temporal scales, which need to be approximated and/or modeled. The presence of density stratification complicates matters further, and gives rise to additional flow modeling and simulation challenges.

Aiming to accurately simulate high-Reynolds-number stratified flows in complex-geometry configurations, in the present work, we develop a new residual-based variational multiscale (RBVMS) formulation for stratified incompressible turbulent flows. RBVMS was first proposed in [4] for large-eddy simulations (LES) of unstratified incompressible turbulent flows. Since then, several research contributions [3,8,16,22,44,51] showed that RBVMS yielded accurate solutions on meshes with LES-level resolution that converged rapidly to the direct numerical simulation (DNS) results with mesh refinement. These features, combined with geometric flexibility of RBVMS, are particularly attractive for predictive simulation of high-Reynolds-number flows for engineering applications, such as wind-turbine aerodynamics and fluid–structure interaction (FSI) [10,24,33,53], FSI of compliant hydrofoils [2,52], patient-specific cardiovascular FSI [40,42], and bioprosthetic heart valves [26,32].

Recently, a stratified turbulent flow formulation based on the Arbitrary Lagrangian–Eulerian Variational Multiscale (ALE-VMS) framework [7,12,14,15,40–42] was proposed in [11]. The formulation was an extension of RBVMS to moving domains through the ALE [28] technique, which is widely used in applications of flows with moving boundaries and interfaces [13,46–48]. However, in the design of the fine-scale fields it was assumed in [11] that the velocity, pressure, and density fine scales were directly proportional only to the strong residuals of their respective equations. In the present work, borrowing ideas from stabilized methods for advective–diffusive systems and compressible flows [29,30,38,49], we design a new closure model for the fine scales that explicitly accounts for the coupling between the velocity and density fields.

This novel RBVMS formulation is implemented both in the context of the Finite Element Method (FEM) and Isogeometric Analysis

* Corresponding author.
E-mail address: yuri@ucsd.edu (Y. Bazilevs).

http://dx.doi.org/10.1016/j.compfluid.2016.12.004
0045-7930/

(IGA) [19,27]. IGA, in contrast to FEM, makes use of higher-order, smooth basis functions widely employed in Computer Graphics and Computer-Aided Design (CAD) systems. Non-Uniform Rational B-Splines (NURBS) [19,27,36], which were the first computational technology implemented within IGA, are employed in the present work. NURBS, due to their excellent approximation properties [6,20] and the ability to efficiently represent many engineering shapes exactly, are well suited for turbulent-flow simulation in geometrically-complex configurations [3,9].

In Section 2 the governing equations of density-stratified flows are presented. In Section 3 the new RBVMS formulation is developed and stated. In Section 4 a self-propelled turbulent wake and stably stratified turbulent channel flows are simulated using the original and new RBVMS formulations. The former example is computed using linear tetrahedral FEM, while the latter example is computed using NURBS-based IGA. The numerical results indicate that the new RBVMS formulation is more accurate than its' original counterpart. In Section 4 conclusions are drawn.

2. Governing equations of density-stratified flows

Stratified environmental flows are typically modeled using the Navier–Stokes equations of incompressible flows with the addition of a Boussinesq forcing term. We focus on the density-stratified case and state the governing partial differential equations *in the non-dimensional form* as follows:

$$\frac{\partial \boldsymbol{u}}{\partial t} + \boldsymbol{u}\cdot\nabla\boldsymbol{u} - \nabla\cdot\boldsymbol{\sigma} - \boldsymbol{f} - \boldsymbol{f}_b = \boldsymbol{0}, \tag{1}$$

$$\nabla\cdot\boldsymbol{u} = 0, \tag{2}$$

$$\frac{\partial \phi}{\partial t} + \boldsymbol{u}\cdot\nabla\phi - \nabla\cdot\nu_\phi\nabla\phi = 0. \tag{3}$$

In Eqs. (1)–(2) $\boldsymbol{u}$ is the fluid velocity, $\boldsymbol{f}$ is the body force, $\boldsymbol{f}_b$ is the Boussinesq forcing term, $\boldsymbol{\sigma}$ is the stress defined as

$$\boldsymbol{\sigma}(\boldsymbol{u}, p) = -p\boldsymbol{I} + 2\nu\nabla^s\boldsymbol{u}, \tag{4}$$

where $\boldsymbol{I}$ is the identity tensor, p is the pressure, ∇^s is the symmetric gradient operator, $\nu = 1/Re$, and Re is the Reynolds number. In Eq. (3) ϕ is the fluid density and $\nu_\phi = 1/(PrRe)$, where Pr is the Prandtl number. The density ϕ is decomposed into three parts, namely,

$$\phi(\boldsymbol{x}, t) = \rho_0 + \bar{\rho}(x_3) + \rho'(\boldsymbol{x}, t), \tag{5}$$

where ρ_0 is a constant background density, $\bar{\rho}(x_3)$ is a linearly varying field in the direction of gravity, and $\rho'(\boldsymbol{x}, t)$ is the density fluctuation, which depends on time and all spatial directions. Both ρ_0 and $\bar{\rho}(x_3)$ are considered known, and the Boussinesq forcing term in Eq. (1) is given by

$$\boldsymbol{f}_b = -Ri\ \rho'(\boldsymbol{x}, t)\ \boldsymbol{e}_3 = -Ri\ (\phi(\boldsymbol{x}, t) - \bar{\rho}(x_3) - \rho_0)\ \boldsymbol{e}_3, \tag{6}$$

where Ri is the Richardson number, which is a non-dimensional parameter that characterizes the degree of stratification in the flow, and $\boldsymbol{e}_3$ is a Cartesian basis vector pointing in the direction opposite to the gravitational force.

In the case of density stratification Ri is defined as

$$Ri = \frac{N^2D^2}{U^2}, \tag{7}$$

were U and D are the characteristic velocity and length scales, and N is the Brunt–Vaisala or buoyancy frequency [34,39] given by

$$N^2 = -\frac{g}{\rho_0}\frac{\partial\bar{\rho}}{\partial x_3}, \tag{8}$$

where g is the gravitational acceleration magnitude. Note that the definition of the Boussinesq forcing term given by Eqs. (6)–(8) implies that the characteristic density scale is $D\frac{\partial\bar{\rho}}{\partial x_3}$. Also note that the definition given by Eq. (8) is meaningful only in the case of negative vertical density gradient (i.e., lighter fluid on top and heavier fluid on the bottom), which is what defines stable stratification.

Provided the appropriate initial and boundary conditions are specified, the above equations constitute a complete mathematical model of density-stratified flows at the continuous level.

3. The new RBVMS formulation for stratified flows

Let $\mathcal{V}$ denote the trial function space for the velocity-pressure-density triple $\{\boldsymbol{u}, p, \phi\}$, and let $\mathcal{W}$ be the space of test functions for the momentum, continuity and density equations denoted by $\{\boldsymbol{w}, q, \eta\}$. The weak form of the stratified-flow equations is stated as follows: Find $\{\boldsymbol{u}, p, \phi\} \in \mathcal{V}$, such that $\forall\{\boldsymbol{w}, q, \eta\} \in \mathcal{W}$,

$$B(\{\boldsymbol{w}, q, \eta\}, \{\boldsymbol{u}, p, \phi\}) = F(\{\boldsymbol{w}, q, \eta\}). \tag{9}$$

Here, B and F, the semi-linear form and linear functional, respectively, are defined as

$$\begin{aligned} &B(\{\boldsymbol{w}, q, \eta\}, \{\boldsymbol{u}, p, \phi\}) \\ &= \int_\Omega \boldsymbol{w}\cdot\left(\frac{\partial\boldsymbol{u}}{\partial t} + \boldsymbol{u}\cdot\nabla\boldsymbol{u}\right)\,\mathrm{d}\Omega + \int_\Omega \nabla\boldsymbol{w} : \boldsymbol{\sigma}(\boldsymbol{u}, p)\,\mathrm{d}\Omega \\ &\quad - \int_\Omega \boldsymbol{w}\cdot\boldsymbol{f}_b\,\mathrm{d}\Omega + \int_\Omega q\nabla\cdot\boldsymbol{u}\,\mathrm{d}\Omega + \int_\Omega \eta\left(\frac{\partial\phi}{\partial t} + \boldsymbol{u}\cdot\nabla\phi\right)\mathrm{d}\Omega \\ &\quad + \int_\Omega \nabla\eta\cdot\nu_\phi\nabla\phi\,\mathrm{d}\Omega, \end{aligned} \tag{10}$$

$$F(\{\boldsymbol{w}, q, \eta\}) = \int_\Omega \boldsymbol{w}\cdot\boldsymbol{f}\,\mathrm{d}\Omega + \int_{\Gamma_h} \boldsymbol{w}\cdot\boldsymbol{h}\,\mathrm{d}\Gamma + \int_{\Gamma_h^\phi} \eta h\,\mathrm{d}\Gamma, \tag{11}$$

where Ω is the flow domain, Γ_h and Γ_h^ϕ are the subsets of the domain boundary with traction and diffusive-flux boundary conditions, respectively, and $\boldsymbol{h}$ and h are the prescribed traction and diffusive-flux functions, respectively.

In this paper the RBVMS framework [4] is adopted to develop a numerical formulation for the stratified-flow equations. RBVMS relies on the orthogonal decomposition of the trial- and test-function spaces, namely, $\mathcal{V} = \mathcal{V}^h \oplus \mathcal{V}'$ and $\mathcal{W} = \mathcal{W}^h \oplus \mathcal{W}'$, where the objects marked by $'$ denote the spaces of unresolved or fine-scale components of the velocity, pressure, and density fields. With this decomposition, the solution fields are split into two parts, namely,

$$\boldsymbol{u} = \boldsymbol{u}^h + \boldsymbol{u}', \tag{12}$$

$$p = p^h + p', \tag{13}$$

$$\phi = \phi^h + \phi', \tag{14}$$

where the coarse-scale quantities with superscript h are resolved on a given problem mesh.

Substituting the above decomposition into the weak form of the stratified-flow equations given by Eq. (9), and restricting the test functions to reside in the space of coarse scales, yields the following semi-discrete RBVMS formulation: Find $\{\boldsymbol{u}^h, p^h, \phi^h\} \in \mathcal{V}^h$, such that $\forall\{\boldsymbol{w}^h, q^h, \eta^h\} \in \mathcal{W}^h$,

$$B_{VMS}\big(\{\boldsymbol{w}^h, q^h, \eta^h\}, \{\boldsymbol{u}^h, p^h, \phi^h\}\big) = F_{VMS}\big(\{\boldsymbol{w}^h, q^h, \eta^h\}\big), \tag{15}$$

where B_{VMS} and F_{VMS} are given by

$$B_{VMS}\big(\{\boldsymbol{w}^h, q^h, \eta^h\}, \{\boldsymbol{u}^h, p^h, \phi^h\}\big) = B\big(\{\boldsymbol{w}^h, q^h, \eta^h\}, \{\boldsymbol{u}^h, p^h, \phi^h\}\big) - \int_\Omega (\boldsymbol{u}^h \cdot \nabla \boldsymbol{w}^h + \nabla q^h) \cdot \boldsymbol{u}' \, \mathrm{d}\Omega - \int_\Omega \boldsymbol{u}^h \cdot \nabla \eta^h \phi' \, \mathrm{d}\Omega - \int_\Omega \nabla \cdot \boldsymbol{w}^h p' \, \mathrm{d}\Omega + \int_\Omega \boldsymbol{w}^h \cdot (\boldsymbol{u}' \cdot \nabla \boldsymbol{u}^h) \, \mathrm{d}\Omega - \int_\Omega \nabla \boldsymbol{w}^h : \boldsymbol{u}' \otimes \boldsymbol{u}' \, \mathrm{d}\Omega, \quad (16)$$

$$F_{VMS}\big(\{\boldsymbol{w}^h, q^h, \eta^h\}\big) = F\big(\{\boldsymbol{w}^h, q^h, \eta^h\}\big). \quad (17)$$

Following [4,11], the fine-scale velocity, pressure and density fields are modeled in a residual-based fashion as

$$\begin{Bmatrix} \boldsymbol{u}' \\ \phi' \end{Bmatrix} = -\boldsymbol{\tau} \begin{Bmatrix} \boldsymbol{r}_M(\boldsymbol{u}^h, p^h, \phi^h) \\ r_\phi(\boldsymbol{u}^h, \phi^h) \end{Bmatrix}, \quad (18)$$

$$p' = -\tau_C r_C(\boldsymbol{u}^h), \quad (19)$$

where $\boldsymbol{r}_M$, r_C and r_ϕ are the residuals of the momentum, continuity and density equations, respectively, thought of as functions of the coarse-scale variables, and given by

$$\boldsymbol{r}_M(\boldsymbol{u}^h, p^h, \phi^h) = \frac{\partial \boldsymbol{u}^h}{\partial t} + \boldsymbol{u}^h \cdot \nabla \boldsymbol{u}^h - \nabla \cdot \boldsymbol{\sigma}(\boldsymbol{u}^h, p^h) - \boldsymbol{f}^h - \boldsymbol{f}_b^h, \quad (20)$$

$$r_C(\boldsymbol{u}^h) = \nabla \cdot \boldsymbol{u}^h, \quad (21)$$

$$r_\phi(\boldsymbol{u}^h, \phi^h) = \frac{\partial \phi^h}{\partial t} + \boldsymbol{u}^h \cdot \nabla \phi^h - \nabla \cdot \nu_\phi \nabla \phi^h, \quad (22)$$

and $\boldsymbol{\tau}$ and τ_C are the fine-scale parameters discussed in what follows.

3.1. Design of the fine-scale parameters

We deviate from the developments in [4,11], and assume that for the 3D case the velocity fine-scale parameter $\boldsymbol{\tau}$ is no longer a diagonal, but a 4×4 matrix. We borrow ideas from stabilized methods for advective–diffusive systems [29,30,38,49] and design $\boldsymbol{\tau}$ as follows:

$$\boldsymbol{\tau} = \boldsymbol{B}^{-\frac{1}{2}}, \quad (23)$$

where $\boldsymbol{B}$ is a matrix given by

$$\boldsymbol{B} = \boldsymbol{A}_0^2 + \boldsymbol{A}_i G_{ij} \boldsymbol{A}_j + C_I \boldsymbol{K}^2 G_{ij} G_{ij}, \quad (24)$$

with the individual submatrices, $\boldsymbol{A}_0$, $\boldsymbol{A}_i$ and $\boldsymbol{K}$ defined as

$$\boldsymbol{A}_0 = \frac{2}{\Delta t} \boldsymbol{I}_{4\times 4} + \begin{Bmatrix} 0 & 0 & 0 & 0 \\ 0 & 0 & 0 & 0 \\ 0 & 0 & 0 & Ri \\ 0 & 0 & 0 & 0 \end{Bmatrix}, \quad (25)$$

$$\boldsymbol{A}_i = u_i \boldsymbol{I}_{4\times 4}, \quad (26)$$

$$\boldsymbol{K} = \begin{Bmatrix} \nu \boldsymbol{I}_{3\times 3} & 0 \\ 0 & \nu_\phi \end{Bmatrix}. \quad (27)$$

Here Δt is the time-step size and C_I is a positive constant that derives from an appropriate element-wise inverse estimate [23]. Furthermore, G_{ij} is the element metric tensor given by

$$G_{ij} = \frac{\partial \xi_k}{\partial x_i} \frac{\partial \xi_k}{\partial x_j}, \quad (28)$$

where $\partial \xi_k / \partial x_i$ is the Jacobian of the mapping between the parametric element and its physical-domain counterpart. Such element metric tensors are typically employed in FEM and IGA to obtain element length scales needed for the definition of fine-scale parameters (see, e.g., [4]).

The square-root-inverse in Eq. (23) may be computed analytically, and expressed as

$$\boldsymbol{\tau} = \begin{Bmatrix} \tau_M & 0 & 0 & 0 \\ 0 & \tau_M & 0 & 0 \\ 0 & 0 & \tau_M & \overline{\tau} \\ 0 & 0 & 0 & \tau_\phi \end{Bmatrix}, \quad (29)$$

where τ_M and τ_ϕ turn out to be the standard scalar-valued parameters employed in the stabilized and multiscale formulations of incompressible-flow and advection–diffusion equations [17,25,45–47,50],

$$\tau_M = \left(\frac{4}{\Delta t^2} + u_i^h G_{ij} u_j^h + C_I \nu^2 G_{ij} G_{ij} \right)^{-1/2}, \quad (30)$$

$$\tau_\phi = \left(\frac{4}{\Delta t^2} + u_i^h G_{ij} u_j^h + C_I \nu_\phi^2 G_{ij} G_{ij} \right)^{-1/2}, \quad (31)$$

and the off-diagonal term $\overline{\tau}$ is given by

$$\overline{\tau} = -\frac{4Ri/\Delta t}{\tau_M^{-1} \tau_\phi^{-2} + \tau_M^{-2} \tau_\phi^{-1}}. \quad (32)$$

In this work we assume that the pressure fine-scale parameter from Eq. (19) retains its usual definition [4], namely,

$$\tau_C = (G_{ii} \tau_M)^{-1}. \quad (33)$$

Note that in the above equations the Einstein summation convention is adopted, which implies summation is taken over all the repeated indices.

Remark. Construction of the velocity fine scales presented above explicitly accounts for the coupling of the Navier–Stokes and density equations through the Boussinesq term. This coupling is reflected in the definition of the $\boldsymbol{A}_0$ matrix in Eq. (25), and gives rise to a non-diagonal $\boldsymbol{\tau}$ in Eq. (23).

Remark. The off-diagonal component of $\boldsymbol{\tau}$ given by Eq. (32) is proportional to Ri. In the case of no stratification, $Ri = 0$, and the formulation automatically reverts to the original RBVMS technique with a diagonal $\boldsymbol{\tau}$.

Remark. In the present work, the new RBVMS formulation of stratified flows is presented on a stationary domain. See [11,43] for the comparable ALE-VMS and ST-VMS formulations for stratified incompressible flows on a moving domain. Extension of the present methodology to the moving-domain case is straightforward.

4. Numerical examples

In this section we present two stratified turbulent-flow examples: A spatially-evolving self-propelled wake and a pressure-driven channel flow. In the former case, linear-tetrahedral FEM is employed for the spatial discretization, while in the latter case the RBVMS formulation is discretized using NURBS-based IGA. This ability to accommodate very different spatial discretizations is viewed as one of the most attractive features of the RBVMS formulation. In the computations presented, the stratified-flow equations are advanced in time using the generalized-α method [5,18,31]. The resulting nonlinear-equation systems are solved using the Newton–Raphson technique, and GMRES with block-diagonal preconditioning [37] is employed to solve the linear-equation systems at each nonlinear iteration.

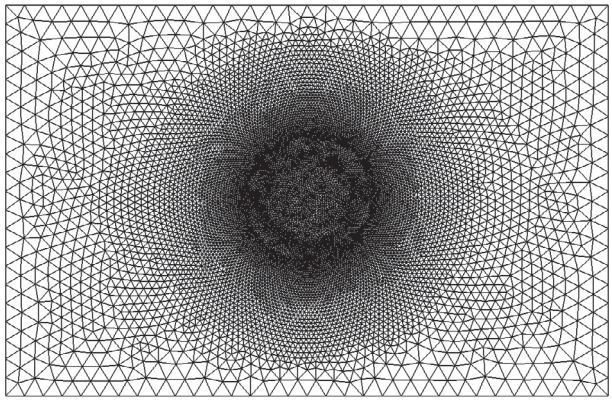

Fig. 1. Spatially-evolving wake. Inlet mesh.

Table 1
Spatially evolving wake. Number of nodes and elements in the spatial computational domain.

	Num. of nodes	Num. of elements
Mesh	3,815,319	22,547,731

Table 2
Spatially-evolving wake. Element sizes employed.

Inner cone	Outer cone	Outer box
0.08	0.1	0.25

4.1. Spatially-evolving self-propelled turbulent wake at $Re = 15,000$

In this section, a spatially evolving wake at $Re = 15,000$, $Ri = 1/9$, and $Pr = 1$ is simulated using the new RBVMS technique. As in the original reference [35], we refer to this case as SP50, which denotes spatially-evolving model of a self-propelled wake with 50% mean kinetic energy with a given energy spectrum. The DNS and original RBVMS simulations of this test case were performed in [35] and [11], respectively. The problem setup, parameters, boundary conditions, mesh size, and time-step size employed in the present simulation are the same as in the original RBVMS simulation from [11], and are briefly summarized below.

The computational domain is a box with dimensions 22.125 D × 14.482 D × 65 D, where D is the characteristic length. The boundary conditions are set as follows. At the inlet, the inflow velocity and density are prescribed. The inflow data is generated by a standalone computation of a temporally evolving wake, which is carried out using a structured-grid finite-volume technique. At the outlet, zero-traction boundary conditions are imposed. On the lateral boundaries, no-penetration and zero-tangential-traction boundary conditions are set for the Navier–Stokes equations, and flux boundary conditions consistent with the background density stratification are imposed for the density equation.

In the computational domain, two refined coaxial cones are built to better capture the stratified turbulent wake. The radii of the inner and outer cones at the inlet are 2.5 D and 3.5 D, respectively, and at the outlet are 3.5 D and 6 D, respectively. The size of the refined region is sufficient to contain the expanding wake. The inlet and planar cut at $y = 0$ of the computational mesh are depicted in Figs. 1 and 2. The mesh statistics are summarized in Tables 1 and 2. The time step is set to $\Delta t = 0.002$.

Fig. 3 shows the instantaneous internal gravity wave field visualized using streamwise vorticity ω_1 contours at $x_1 = 46.11$. The RBVMS simulations are able to replicate the gravity-wave patterns, such as pancake-like vortices, which are present in the DNS results. However, as is evident from the figure, the results of the new RBVMS formulation show more pronounced vorticity lobes, and are visually in much better agreement with the DNS data than the results of the original RBVMS formulation. Fig. 4 shows the plane-integrated turbulent production and normalized turbulent kinetic energy plotted as a function of the streamwise coordinate x_1. Good agreement is achieved between the RBVMS simulations and the DNS results. For the quantities presented, differences between the new and original RBVMS results are not as pronounced, except for integrated production in the region around $x_1 = 20$, where the new RBVMS formulation shows significant improvement over its original counterpart. Velocity magnitude on several planes along the streamwise direction is visualized in Fig. 5. The turbulent wake expands in both vertical and spanwise directions. Eddies are formed and travel to the boundary in the downstream direction, displaying complex flow behavior.

4.2. Pressure-driven turbulent channel flow at $Re_\tau = 180$

We compute the problem of stratified turbulent channel flow. The flow is characterized by dimensionless friction Reynolds and Richardson numbers, Re_τ and Ri_τ, respectively, which are defined as $Re_\tau = u_\tau \delta/\nu$ and $Ri_\tau = \Delta\rho g\delta/\rho_0 u_\tau^2$. Here u_τ is the friction velocity, δ is the channel half-height, $\Delta\rho$ is the difference in the density values between the channel walls, and g is the gravitational acceleration. The flow is driven by a constant pressure gradient along the streamwise direction. A stable stratification is enforced by setting a higher constant density at the bottom wall, and a lower constant density at the top wall. We set $Re_\tau = 180$ and $Pr = 0.71$. An unstratified case with $Ri_\tau = 0$ and a stratified case with $Ri_\tau = 18$ are computed using both formulations. (Note that the original and new RBVMS formulations are identical for the case of $Ri_\tau = 0$.) The computational domain, depicted in Fig. 6, is a box with dimensions $4\pi \times \frac{4}{3}\pi \times 2$ discretized using 48 × 64 × 64 quadratic NURBS elements in the streamwise, spanwise, and wall-normal directions, respectively. The time step is set to $\Delta t = 0.025$. The RBVMS results are compared with the fine-grid LES of [1] and the DNS of [21] when possible.

Fig. 7 shows the ensemble-averaged streamwise velocity and density as functions of the wall-normal coordinate. In the figure, the velocity is scaled by u_{c0}, which is the mean centerline streamwise velocity for the case with no stratification (i.e., $Ri_\tau = 0$), while the density is shifted by ρ_{cl}, the mean centerline density of the unstratified case, and normalized by $\Delta\rho$. For the unstratified case, excellent agreement between the RBVMS, the LES of [1] and DNS of [21] is achieved for both mean velocity and density. For the stratified case, close to the walls, the RBVMS results agree with the LES and DNS very well. In the channel core, however, some deviation is observed between the original RBVMS and LES and DNS results of [1,21], respectively, while the results produced by the new RBVMS formulation are in excellent agreement with the LES and DNS. These results show a clear advantage of the new RBVMS formulation over its original counterpart for stratified turbulent flows.

Fig. 8 shows the root-mean-square (RMS) of streamwise velocity and density as functions of the wall-normal coordinate. Only the results of the stratified case $Ri_\tau = 18$ are reported. The velocity fluctuations are normalized using the channel bulk velocity u_b, while the density fluctuations are normalized by $\Delta\rho$. Relative to the LES of [1], the new RBVMS gives more accurate results than the original RBVMS. The differences are most pronounced for the RMS of density, where the original RBVMS underpredicts the fluctuation by nearly 25% in the channel core. Continuing with density RMS, the newly introduced RBVMS method is in better agreement with the LES of [1] than the DNS of [21]. This is expected given that the RBVMS simulation is closer to an LES than a DNS. Meanwhile the streamwise velocity RMS obtained with the new RBVMS

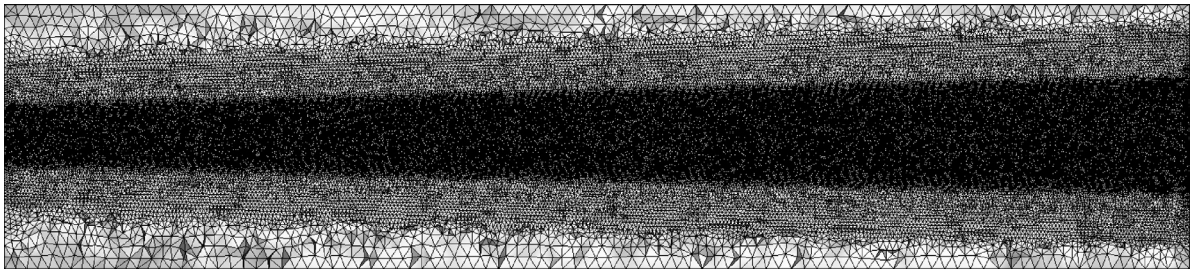

Fig. 2. Spatially-evolving wake. Mesh of a planar cut at $y = 0$.

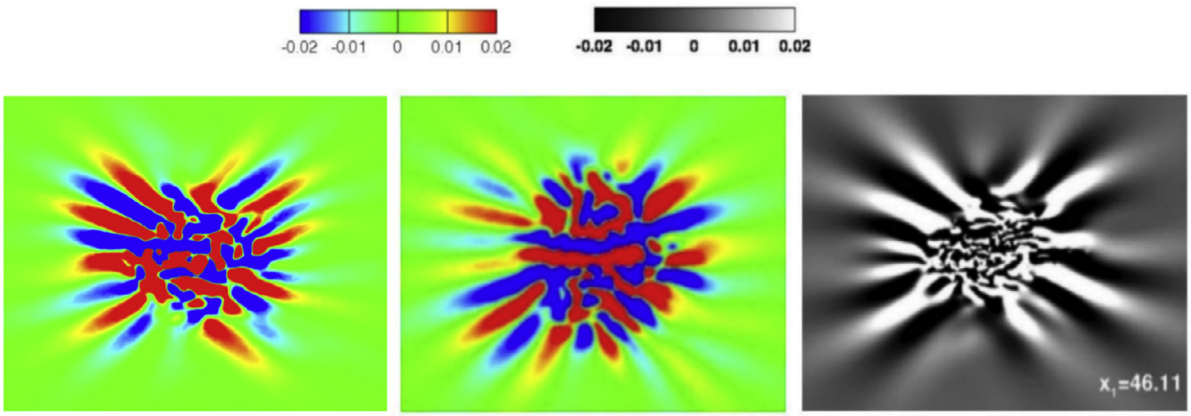

Fig. 3. Spatially evolving wake. Contours of streamwise vorticity at $x_1 = 46.11$; Left: New RBVMS. Middle: Original RBVMS [11]. Right: DNS [35].

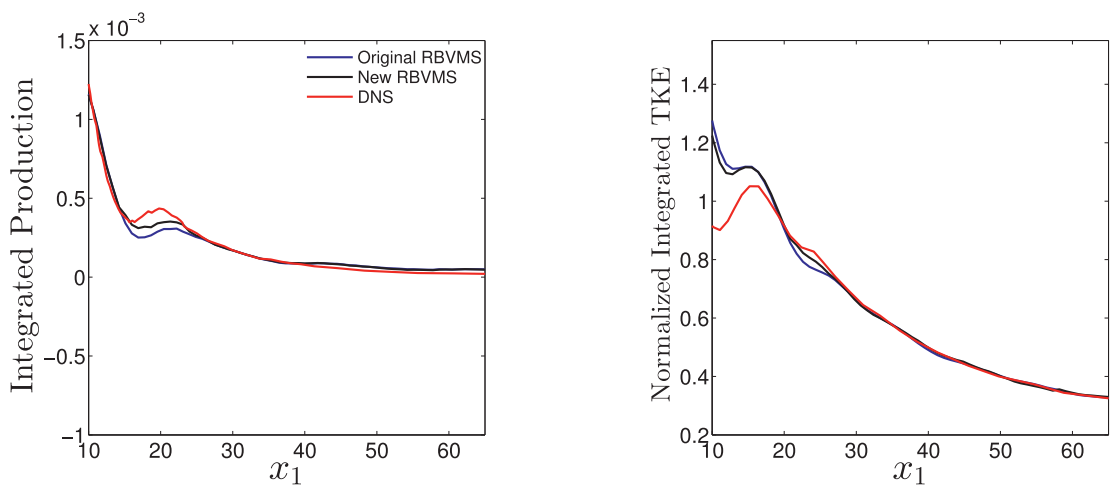

Fig. 4. Spatially evolving wake. Plane-integrated turbulence statistics as a function of streamwise coordinate x_1. Left: Turbulent production; Right: Normalized turbulent kinetic energy.

method displays similar structure to the streamwise velocity RMS from the LES [1] and the DNS [21] in the bulk flow region ($x_3/\delta > 0.4$), where all three RMS profiles follow a near-linear profile for most this range (except at mid-height, $x_3/\delta = 1$). This is in contrast with the velocity RMS profile obtained with the original RBVMS method which misses this near-linear behavior displaying a pronounced curvature up to $x_3/\delta = 1$.

In terms of spanwise and wall-normal velocity RMS (normalized using the channel bulk velocity u_b), Fig. 9 shows that the new RBVMS gives more accurate results than the original RBVMS throughout the majority of the channel depth.

In addition to simulations at $Ri_\tau = 18$, corresponding to a weakly stably stratified regime, [21] and [1] have conducted simulations at Ri_τ much greater than 18. Stably stratified channel flow simulations at $Re_\tau > 180$ were also performed in [21]. However, even at the relatively low stratification corresponding to $Ri_\tau = 18$, the stratification induces significant changes to mean velocity and density fields and related higher order statistics, as observed above. Furthermore, even at this relatively low stratification, the trajectory of simulations are significantly different than the unstratified case due to the tendency of the stratification to initially suppress the turbulence. This suppression can last over on the order of one or more flow-throughs, but eventually the turbulence re-ignites leading to a stably stratified turbulent regime (see [1] for details of the initial suppression of the turbulence). In our experience, the original RBVMS method on LES grids can lead to suppression of the turbulence over longer periods than the new RBVMS. Future research should focus on the physical significance of this initial suppression of the turbulence and how the different LES subgrid-scale models behave during this stage. Future research

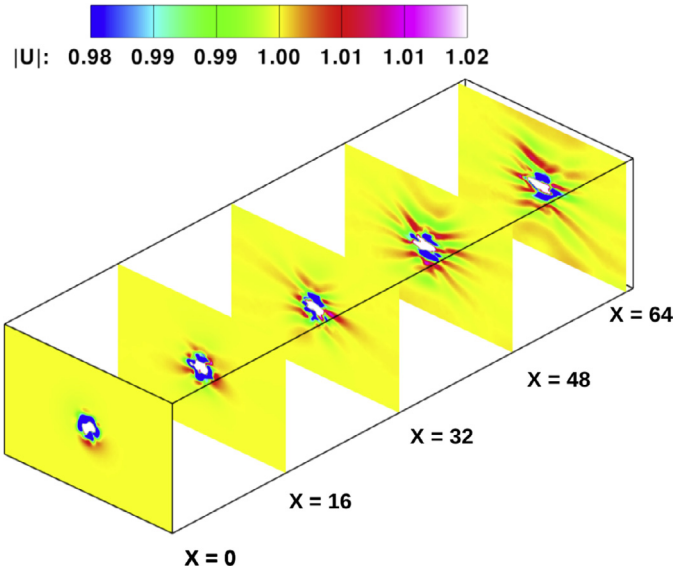

Fig. 5. Spatially evolving wake. Velocity magnitude on several planes along the streamwise direction.

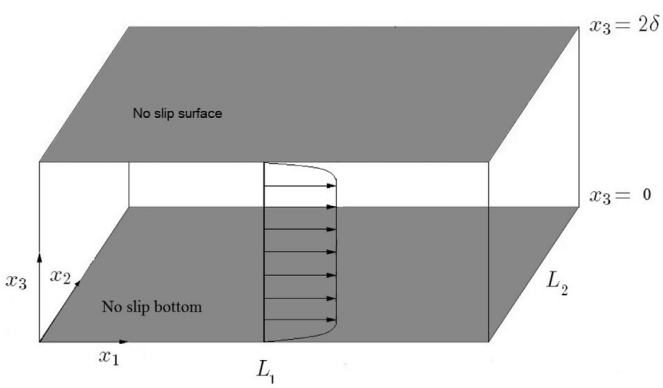

Fig. 6. Turbulent channel flow. Problem domain.

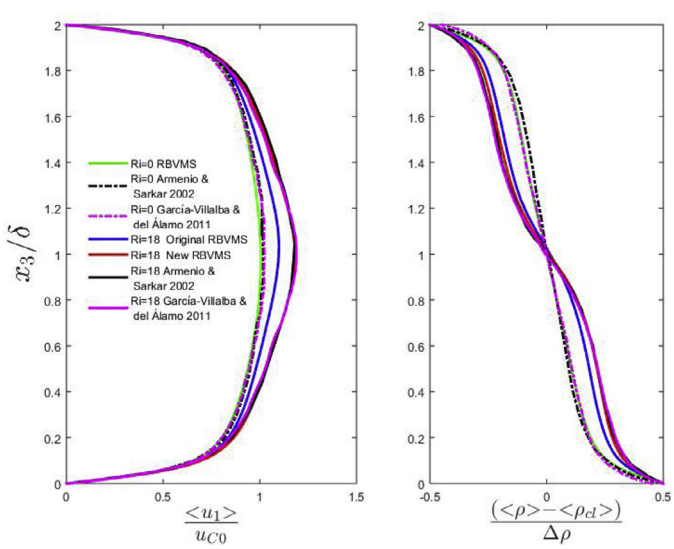

Fig. 7. Turbulent channel flow. a) Ensemble-averaged streamwise velocity as a function of the wall-normal coordinate; b) Ensemble-averaged density as a function of the wall-normal coordinate. RBVMS results are compared with the LES data of [1].

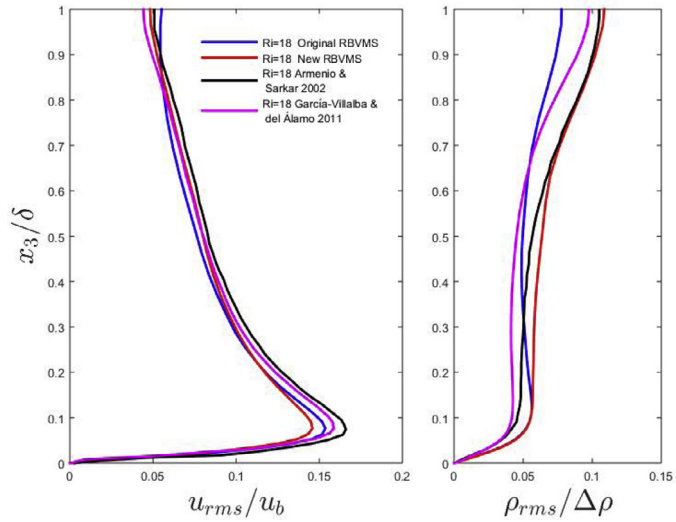

Fig. 8. Turbulent channel flow. a) RMS of velocity and b) density as functions of the wall-normal coordinate. RBVMS results are compared with the LES data of [1] and the DNS data of [21].

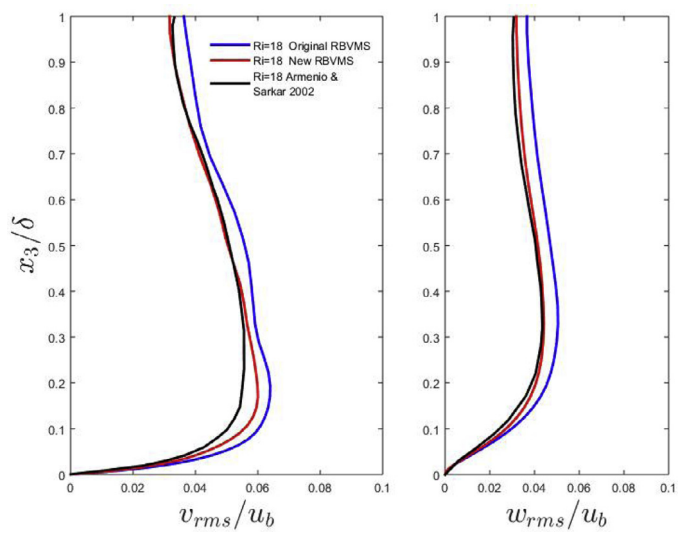

Fig. 9. Turbulent channel flow. a) RMS of spanwise velocity and b) wall-normal velocity as functions of the wall-normal coordinate. RBVMS results are compared with the LES data of [1].

should also assess the new RBVMS formulation at $Re_\tau > 180$ for which the work of [21] has uncovered new physics not present in the $Re_\tau = 180$ case.

5. Conclusions

A new numerical formulation for stably-stratified turbulent flows is developed using the framework of RBVMS methods. Using ideas from stabilized methods for convective–diffusive systems and compressible flows, a new closure model for the fine scales is proposed that introduces coupling between the velocity fine scales and density-equation residual. The new formulation was tested on two turbulent-flow examples and showed good agreement with the DNS and fine-grid LES results reported by other researchers. Although the new RBVMS formulation only adds one term to the velocity fine scales that is based on the residual of the density equation, this seemingly small change shows a relatively large accuracy improvement over the traditional RBVMS, in which the velocity, pressure, and density fine scales are proportional only to

the strong residuals of their respective equations. Because this new term scales with Richardson number, its positive effect is more pronounced with increasing density stratification, as evidenced by the numerical results presented.

Acknowledgements

This work was partially supported by the NSF CAREER Awards 1055091 and 0846510, and NSF Award CBET-1306869. This support is gratefully acknowledged.

References

[1] Armenio V, Sarkar S. An investigation of stably stratified turbulent channel flow using large-eddy simulation. J Fluid Mech 2002;459:1–42.
[2] Augier B, Yan J, Korobenko A, Czarnowski J, Ketterman G, Bazilevs Y. Experimental and numerical FSI study of compliant hydrofoils. Comput Mech 2015;55:1079–90.
[3] Bazilevs Y, Akkerman I. Large eddy simulation of turbulent Taylor–Couette flow using isogeometric analysis and the residual–based variational multiscale method. J Comput Phys 2010;229:3402–14.
[4] Bazilevs Y, Calo VM, Cottrel JA, Hughes TJR, Reali A, Scovazzi G. Variational multiscale residual-based turbulence modeling for large eddy simulation of incompressible flows. Comput Methods Appl Mech Eng 2007;197:173–201.
[5] Bazilevs Y, Calo VM, Hughes TJR, Zhang Y. Isogeometric fluid–structure interaction: theory, algorithms, and computations. Comput Mech 2008;43:3–37.
[6] Bazilevs Y, Veiga LBd, Cottrell JA, Hughes TJR, Sangalli G. Isogeometric analysis: approximation, stability and error estimates for h-refined meshes. Math Models Methods Appl Sci 2006;16:1031–90.
[7] Bazilevs Y, Hsu M-C, Takizawa K, Tezduyar TE. ALE-VMS and ST-VMS methods for computer modeling of wind-turbine rotor aerodynamics and fluid–structure interaction. Math Models Methods Appl Sci 2012;22(supp02):1230002.
[8] Bazilevs Y, Hughes TJR. Weak imposition of Dirichlet boundary conditions in fluid mechanics. Comput Fluids 2007;36:12–26.
[9] Bazilevs Y, Hughes TJR. NURBS-based isogeometric analysis for the computation of flows about rotating components. Comput Mech 2008;43:143–50.
[10] Bazilevs Y, Korobenko A, Deng X, Yan J. Fluid–structure interaction modeling for fatigue-damage prediction in full-scale wind-turbine blades. J Appl Mech 2016;83(6):061010.
[11] Bazilevs Y, Korobenko A, Yan J, Pal A, Gohari SMI, Sarkar S. ALE-VMS formulation for stratified turbulent incompressible flows with applications. Math Models Methods Appl Sci 2015;25:1540011.
[12] Bazilevs Y, Takizawa K, Tezduyar TE. Challenges and directions in computational fluid–structure interaction. Math Models Methods Appl Sci 2013;23:215–21.
[13] Bazilevs Y, Takizawa K, Tezduyar TE. Computational fluid–Structure interaction: methods and applications. Wiley; 2013.
[14] Bazilevs Y, Takizawa K, Tezduyar TE. New directions and challenging computations in fluid dynamics modeling with stabilized and multiscale methods. Math Models Methods Appl Sci 2015;25:2217–26.
[15] Bazilevs Y, Takizawa K, Tezduyar TE, Hsu M-C, Kostov N, McIntyre S. Aerodynamic and FSI analysis of wind turbines with the ALE-VMS and ST-VMS methods. Arch Comput Methods Eng 2014;21:359–98.
[16] Bazilevs Y, Yan J, de Stadler M, Sarkar S. Computation of the flow over a sphere at Re = 3700: a comparison of uniform and turbulent inflow conditions. J Appl Mech 2014;81(12):121003.
[17] Brooks AN, Hughes TJR. Streamline upwind/Petrov-Galerkin formulations for convection dominated flows with particular emphasis on the incompressible Navier-Stokes equations. Comput Methods Appl Mech Eng 1982;32:199–259.
[18] Chung J, Hulbert GM. A time integration algorithm for structural dynamics withimproved numerical dissipation: the generalized-α method. J Appl Mech 1993;60:75–371.
[19] Cottrell JA, Hughes TJR, Bazilevs Y. Isogeometric analysis: toward integration of CAD and FEA. Chichester: Wiley; 2009.
[20] Veiga LBd, Cho D, Sangalli G. Anisotropic NURBS approximation in isogeometric analysis. Comput Methods Appl Mech Eng 2012;209–212:1–11.
[21] García-Villalba M, Álamo JCd. Turbulence modification by stable stratification in channel flow. Phys Fluids 2011;23:045104.
[22] Golshan R, Tejada-Martínez AE, Juha M, Bazilevs Y. Large-eddy simulation with near-wall modeling using weakly enforced no-slip boundary conditions. Comput Fluids 2015;118:172–81.
[23] Harari I, Hughes TJR. What are C and h?: Inequalities for the analysis and design of finite element methods. Comput Methods Appl Mech Eng 1992;97:157–92.
[24] Hsu M-C, Akkerman I, Bazilevs Y. Finite element simulation of wind turbine aerodynamics: Validation study using NREL Phase VI experiment. Wind Energy 2014;17:461–81.
[25] Hsu M-C, Bazilevs Y, Calo VM, Tezduyar TE, Hughes TJR. Improving stability of stabilized and multiscale formulations in flow simulations at small time steps. Comput Methods Appl Mech Eng 2010;199:828–40.
[26] Hsu M-C, Kamensky D, Bazilevs Y, Sacks MS, Hughes TJR. Fluid–structure interaction analysis of bioprosthetic heart valves: significance of arterial wall deformation. Comput Mech 2014;54:1055–71.
[27] Hughes TJR, Cottrell JA, Bazilevs Y. Isogeometric analysis: CAD, finite elements, NURBS, exact geometry, and mesh refinement. Comput Methods Appl Mech Eng 2005;194:4135–95.
[28] Hughes TJR, Liu WK, Zimmermann TK. Lagrangian–Eulerian finite element formulation for incompressible viscous flows. Comput Methods Appl Mech Eng 1981;29:329–49.
[29] Hughes TJR, Mallet M. A new finite element formulation for computational fluid dynamics: III. The generalized streamline operator for multidimensional advective-diffusive systems. Comput Methods Appl Mech Eng 1986;58:305–28.
[30] Hughes TJR, Scovazzi G, Tezduyar TE. Stabilized methods for compressible flows. J Sci Comput 2010;43:343–68. doi:10.1007/s10915-008-9233-5.
[31] Jansen KE, Whiting CH, Hulbert GM. A generalized-α method for integrating the filtered Navier-Stokes equations with a stabilized finite element method. Comput Methods Appl Mech Eng 2000;190:305–19.
[32] Kamensky D, Hsu M-C, Schillinger D, Evans JA, Aggarwal A, Bazilevs Y, et al. An immersogeometric variational framework for fluid–structure interaction: Application to bioprosthetic heart valves. Comput Methods Appl Mech Eng 2015;284:1005–53.
[33] Korobenko A, Hsu M-C, Akkerman I, Bazilevs Y. Aerodynamic simulation of vertical-axis wind turbines. J Appl Mech 2013;81(2):021011.
[34] Kundu P, Cohen I. Fluid mechanics. 2nd ed. Elsevier; 2002.
[35] Pal A, de Stadler MB, Sarkar S. The spatial evolution of fluctuations in a self-propelled wake compared to a patch of turbulence. Phys Fluids 2013;25(9):095106.
[36] Piegl L, Tiller W. The NURBS book (monographs in visual communication). 2nd ed. New York: Springer-Verlag; 1997.
[37] Saad Y, Schultz M. GMRES: a generalized minimal residual algorithm for solving nonsymmetric linear systems. SIAM J Sci Stat Comput 1986;7:856–69.
[38] Shakib F, Hughes TJR, Johan Z. A multi-element group preconditioned GMRES algorithm for nonsymmetric systems arising in finite element analysis. Comput Methods Appl Mech Eng 1989;75:415–56.
[39] Sutherland B. Internal wave propagation. Modern applied mathematics. New Delhi: Narosa Press; 2005.
[40] Takizawa K, Bazilevs Y, Tezduyar TE. Space–time and ALE-VMS techniques for patient-specific cardiovascular fluid–structure interaction modeling. Arch Comput Methods Eng 2012;19:171–225.
[41] Takizawa K, Bazilevs Y, Tezduyar TE, Hsu M-C, Øiseth O, Mathisen KM, et al. Engineering analysis and design with ALE-VMS and space–time methods. Arch Comput Methods Eng 2014;21:481–508.
[42] Takizawa K, Bazilevs Y, Tezduyar TE, Long CC, Marsden AL, Schjodt K. ST and ALE-VMS methods for patient-specific cardiovascular fluid mechanics modeling. Math Models Methods Appl Sci 2014;24:2437–86.
[43] Takizawa K, Tezduyar TE, Kuraishi T. Multiscale ST methods for thermo-fluid analysis of a ground vehicle and its tires. Math Models Methods Appl Sci 2015;25:2227–55.
[44] Tejada-Martínez AE, Akkerman I, Bazilevs Y. Large-eddy simulation of shallow water langmuir turbulence using isogeometric analysis and the residual-based variational multiscale method. J Appl Mech 2012;79(1):010909.
[45] Tezduyar T, Sathe S. Stabilization parameters in SUPG and PSPG formulations. J Comput Appl Mech 2003;4:71–88.
[46] Tezduyar TE. Computation of moving boundaries and interfaces and stabilization parameters. Int J Numer Methods Fluids 2003;43:555–75.
[47] Tezduyar TE. Finite element methods for fluid dynamics with moving boundaries and interfaces. Encyclopedia of computational mechanics, vol 3. John Wiley & Sons; 2004. Fluids, chapter 17
[48] Tezduyar TE. Finite elements in fluids: stabilized formulations and moving boundaries and interfaces. Comput Fluids 2007;36:191–206.
[49] Tezduyar TE, Hughes TJR. Finite element formulations for convection dominated flows with particular emphasis on the compressible Euler equations. In: Proceedings of AIAA 21st aerospace sciences meeting; 1983. AIAA Paper 83–0125, Reno, Nevada
[50] Tezduyar TE, Mittal S, Ray SE, Shih R. Incompressible flow computations with stabilized bilinear and linear equal-order-interpolation velocity-pressure elements. Comput Methods Appl Mech Eng 1992;95:221–42.
[51] Xu F, Schillinger D, Kamensky D, Varduhn V, Wang C, Hsu M-C. The tetrahedral finite cell method for fluids: immersogeometric analysis of turbulent flow around complex geometries. Comput Fluids 2015. doi:10.1016/j.compfluid.2015.08.027.
[52] Yan J, Augier B, Korobenko A, Czarnowski J, Ketterman G, Bazilevs Y. FSI modeling of a propulsion system based on compliant hydrofoils in a tandem configuration. Comput Fluids 2015. doi:10.1016/j.compfluid.2015.07.013.
[53] Yan J, Korobenko A, Deng X, Bazilevs Y. Computational free-surface fluid-structure interaction with application to floating offshore wind turbines. Comput Fluids 2016. doi:10.1016/j.compfluid.2016.03.008.